AIAA SciTech
4-8 January 2016, San Diego, California, USA
3rd AIAA Spacecraft Structures Conference

UltraFlex and MegaFlex – Advancements in Highly Scalable Solar Power

David M. Murphy,[1] Michael I. Eskenazi,[2] Michael E. McEachen,[3] and James W. Spink[4]
Orbital ATK, Space Components Division, Deployables Segment, 600 Pine Ave, Goleta, CA 93117

This paper details NASA Game Changing Development (GCD) program efforts to evolve heritage Orbital ATK UltraFlex spacecraft solar power technology to support *much higher* power-level applications. The resulting MegaFlex wing employs enhanced UltraFlex technology to enable very high power solar electric propulsion (SEP) missions through the introduction of spar-folding joints and associated extension panel hinges into the UltraFlex solar array system (SAS). These advances enable much greater deployed solar array area to be launched from a given spacecraft volume allocation compared to UltraFlex, since the largest dimension (stowed length) is significantly reduced. The subject GCD SEP-SAS program activity, begun in October of 2012, was managed by Glenn Research Center (GRC). By April of 2014 the team was successful in maturing MegaFlex to a Technology Readiness Level (TRL) of 5+ and had completed validation testing of a flight-fidelity 10-m-diameter wing at the NASA-GRC Plum Brook Station. The MegaFlex wing, which demonstrated extremely high performance in specific power, strength, stiffness, stowed compaction and scalability, is uniquely well suited to a wide range of mission power levels, such as 30–50 kW near-term SEP applications and up to 300-kW future systems and beyond.

I. Introduction

MegaFlex is an evolution of heritage UltraFlex solar array technology, with additions that enhance the compaction for stowage to allow affordable launch of very high-power spacecraft. With just two wings packaged on a SEP vehicle within a (single) Falcon fairing, over 300 kW can be delivered to orbit, meaning MegaFlex allows 50% more power than all eight wings on the International Space Station in just *one* launch. Given the remarkable performance of UltraFlex and MegaFlex – *low mass, compact stowage, high stiffness, and high strength* – together with scalability from 1 kW to over 400 kW, this technology is applicable to a wide-ranging set of missions.

MegaFlex achieves similar performance characteristics to UltraFlex over this entire power range, with specific power up to 200 W/kg, depending on specific mission requirements.

MegaFlex technology clearly supports NASA's roadmap for SEP mission power growth. The MegaFlex wing design has a straightforward extensibility path via direct scaling, rather than duplication of deployable winglets along an additional deployable structure, providing the minimum-risk and highest-reliability path to very high power levels.

The simplicity of direct scaling allows full system end-to-end deployment validation in

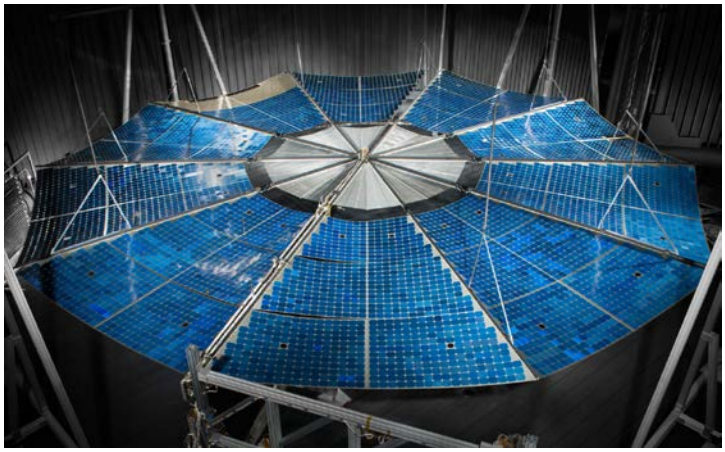

Figure 1. 10-m MegaFlex Demonstration Unit (MDU) Wing.

[1] Director of Engineering, Orbital ATK, 600 Pine Ave, Goleta, CA, AIAA Senior Member.
[2] Director of Operations, Orbital ATK, 600 Pine Ave, Goleta, CA.
[3] Technical Director, Orbital ATK, 600 Pine Ave, Goleta, CA, AIAA Member.
[4] Program Manager, Orbital ATK, 600 Pine Ave, Goleta, CA.

existing space environmental test facilities, namely the GRC Space Power Facility at Plum Brook Station.

The subject SEP-SAS program activity, performed by ATK Space Systems in Goleta, California (now Orbital ATK), and our partners under a NASA Game Changing Development (GCD) program managed by NASA GRC, has been successful in rapidly maturing MegaFlex to a Technology Readiness Level (TRL) of 5+. MegaFlex effectively meets the emerging need for high power SEP technology with true scalability, offering a high-performance solution that uniquely allows for complete ground test and validation of 20 to 400 kW array system wings in existing space environment test facilities.

A. Background

Fifty years ago America created rockets large enough to take us to the moon, but we have not sent anyone farther, or even as far, since. Although launching into space is now almost routine, few spacecraft have had the capability to substantially change their own trajectory. With the launch of Deep Space 1 in 1998, NASA began a new era of possibilities for exploration of the solar system. For 16,000 hours, a revolutionary ion engine, powered by a concentrator solar array built by Orbital ATK - Goleta (OAG), ejected xenon ions at 25 miles per second, slowly adding acceleration with a mass efficiency 10 times that of conventional rocket engines.[1] DS1, with solar wings that spread 48 feet tip-to-tip to produce 2,500 watts,[2] traveled to 1.6 AU and caught close-up views of a comet. NASA took a second leap forward in solar electric propulsion in 2007, with the launch of the Dawn spacecraft (built by Orbital ATK). The three ion engines on Dawn together with a 10-kW solar array, have propelled the spacecraft to targets in the asteroid belt (as far at 3 AU)[3] with a net velocity change of over 10 km/s – far more than any other spacecraft has done using conventional chemical engines.

Larger ion engines – and larger solar array systems to power them – are key elements for America's future in space. NASA's strategic roadmaps for exploration, science, and advanced technology all consider SEP an essential capability to develop further… so that we may go farther.

Many NASA missions road-mapped by the Science Mission Directorate (SMD) and documented in the most recent decadal survey[4] plan to employ SEP. UltraFlex wings are baselined as the power generation system for the majority of these missions due to the high performance and flight heritage of the technology. The Human Exploration and Operations Mission Directorate (HEO) plans for much larger SEP architectures – with massive solar array systems – that will one day help support a sustainable, affordable human presence in space. NASA-GRC has led the way in the development of SEP system technologies through mission studies[5-8] and technology development management,[9] including the activity that is the subject of this paper (and an earlier abbreviated publication[10]), which began as a proposal to NASA Research Announcement (NRA) NNL12A3001N[11] from the Office of Chief Technologist's Game Changing Development (GCD) program.

B. Program Overview

The NASA GCD SEP-SAS program targeted development of new solar array systems capable of supporting SEP applications at power levels from 25 kW to 250 kW. OAG recognized the scaling potential of UltraFlex[12] and proposed to build upon and extend our heritage UltraFlex technology to meet the challenges put forth by the NRA. The Phase I effort succeeded in maturing the MegaFlex SAS concept to TRL 5+ in support of future 30 to 50-kW SEP applications while being challenged to develop analytical methods to scale the concept to a total system power level of 250 kW or greater. The technology development effort successfully produced an integrated design for all electrical and mechanical systems, demonstrated with a flight-like 10-m-diameter wing.

Hardware development was phased to first build and test new mechanical subassemblies and photovoltaic coupons to best mitigate risk and allow design evolution based on test findings. Engineering activities included, but were not limited to, creation and trading of new and evolved subsystem mechanism designs (See Section II), structural and thermal analyses (See Section III), power production analysis, photovoltaic (PV) coupon development for high voltages in a SEP plasma environment, and power management (harnessing) hardware validation (See Section IV). All of these activities are critical elements of the total program effort aligned to rapidly develop MegaFlex and validate performance against the program requirements. Section V provides a review of the results against the top-level requirements, such as W/kg, kW/m^3, stiffness, and strength.

Executing *and learning from* the MegaFlex Development Unit (MDU) test series were the culminating activities for the program. This extended activity took place at the NASA-GRC Plum Brook Station Space Power Facility.[13] The testing activities spanned January to April in 2014, and the results were reviewed in detail in the System Definition Review (SDR), the final program review, on April 29th at GRC. A narrative overview of the test program and key findings is presented in Section VI. Near the end of the program the focus shifted to the investigation of the scalability of the validated technology (See Section VII) and production of the final report, from which much of the content of this paper is drawn.

The program began with a kickoff meeting with NASA in October of 2012 and co-development of a complete set of specifications for SAS performance that were reviewed and agreed upon at the Systems Requirements Review (SRR) meeting in November. After the design progressed substantially, an interim MDU Design Review (MDUDR) was held in May of 2013 to discuss the development of the wing design and receive approval for initiation of long lead procurements via a concurrent Manufacturing Readiness Review (MRR).

The developmental elements required to enable extension of the folded-back spars were demonstrated early in the program with a dedicated test bed termed the Folding Subsystem Pathfinder (FSP). High fidelity analytical models of the entire wing were produced in concert with the 10-m-diameter ground test article design. These models were validated by component/subsystem test data with the FSP elements in order to reduce modeling uncertainty.

By November 2013, 13 months after starting the program, OAG had the MDU wing build activity nearly completed and a Test Readiness Review (TRR) was held. The primary program objective was to maximize technology development, and as such, program controls and quality systems typically applied to qualification hardware were tailored appropriately in the fabrication and testing of the hardware.

The SEP-SAS development effort was intended to occur in two phases. Phase 1 was planned to advance the TRL of all critical systems up to or beyond level 5 over a period of 18 months, and OAG successfully completed that top level goal within budget constraints. Phase 1 concluded with the SDR meeting in April of 2014. Phase 2 was planned to be a demonstration mission of critical SEP technologies (e.g. references 14–16), but based on the success of Phase 1, other options came under consideration instead – including providing power to the Asteroid Redirect Mission, the first in a series of missions leading to manned missions to an asteroid, Mars, or other destinations.[17]

Many of the subsystems of the MDU were drawn directly from an UltraFlex program that had recently completed protoflight testing (and was scheduled to fly in December of 2015), and therefore were already at TRL 8. The new mechanisms in MegaFlex were advanced to TRL 7 or higher. Despite the high TRL of MegaFlex, NASA has evaluated the TRL at 5+, because two significant aspects remain to be evaluated: (1) PV coupon degradation in a combined exposure test (in a laboratory or on-orbit) to evaluate the potential for *synergistic* degradation from thermal cycling, radiation, UV, plasma, and MMOD environments, and (2) The deployment behavior of the blanket unfurling in a zero-g environment, which was not accurately simulated due to influences of gravity on the tested hardware.

The latter issue was investigated by OAG during the summer of 2014 in a follow-on task for GRC. Methods to better simulate a 0-g environment, and mechanical controls to replicate the organizing influence of gravity on earth into the blanket for flight were successfully developed. The flight of the first UltraFlex wings on the OA-4 mission to the Space Station will provide insight (via video imagery) into 0-g blanket deployment behavior *without* the added mechanical controls developed for much larger MegaFlex wings.

The NASA GRC-managed SEP-SAS program has been successful in advancing MegaFlex technology into a scalable, high-performance, high TRL solar array uniquely suited to a wide range of SEP mission power levels, from 30 to 300 kW systems and beyond.

II. Description of Design

MegaFlex is simply UltraFlex technology enhanced to enable very high-power applications through the introduction of two new features: folding spar joints and panel extension hinges. These features allow stowage in an even more compact volume with the longest-length dimension significantly reduced.

For example, with the spars folded at one-third out from the center, a 30-m-diameter wing will stow for launch with a major dimension of 10 m, which is compatible with the spacecraft anticipated for such a mission. Two wings of this size can provide 450 kW, and they will package in just a small fraction of the fairing volume of launch vehicles under development, as described in further detail in Section XII and depicted in Fig. 17. The potential for power will rise as cell efficiency continues to improve in the coming years. But already, a two-wing MegaFlex array can provide well beyond the 250-kW power-level challenge levied by NASA, on a spacecraft that fits easily in a 4-m fairing launch vehicle.

A scaled configuration is preferred: (1) To avoid the loss in reliability suffered with the "modular" approach of deploying a great number of smaller wings to achieve the area provided by one large wing (along with the associated deployed winglet linking structure), (2) The approach enables *full system* validation testing for small or large systems, and (3) the circular profile naturally provides clearance from the highly energetic main engine plume while minimizing MOI – which is of benefit to strength and frequency performance. For those less familiar with this type of solar array wing (SAW) design, a brief general description of the configuration and function follows.

A. Functional Overview

A MegaFlex SAW can be thought of as consisting of two primary subsystems: the structural *Platform Assembly*, consisting of the composite honeycomb Panels and the radial Spars and connecting mechanism; and the *Power Assembly*, consisting of the photovoltaic-populated Gores. The triangular membrane gores are comprised of smaller gorelets, sized for modularity and manageability. For the 10-m MDU SAW, the 10 folding gores were configured to have 6 gorelets each. The gorelets are formed with a gossamer woven fabric mesh bonded at the edges to thin graphite strips (sparlets), creating a lightweight and manageably-sized substrate for the laydown of photovoltaic (PV) assemblies. Multiple PV strings (interconnected solar cells) and associated circuitries are arranged on each gorelet.

In wing assembly and checkout, completed and tested PV-populated gorelets are brought to a completed Platform Assembly, and the sparlets are hung from and screwed-in below each spar. The spars are cut from sheets of high-modulus graphite fiber in a cyanate-ester resin, with individual plies oriented for optimal bending and torsion performance. Finally, the sparlets along the gore midlines are then joined (with removable fasteners), which completes integration of the Power Assembly.

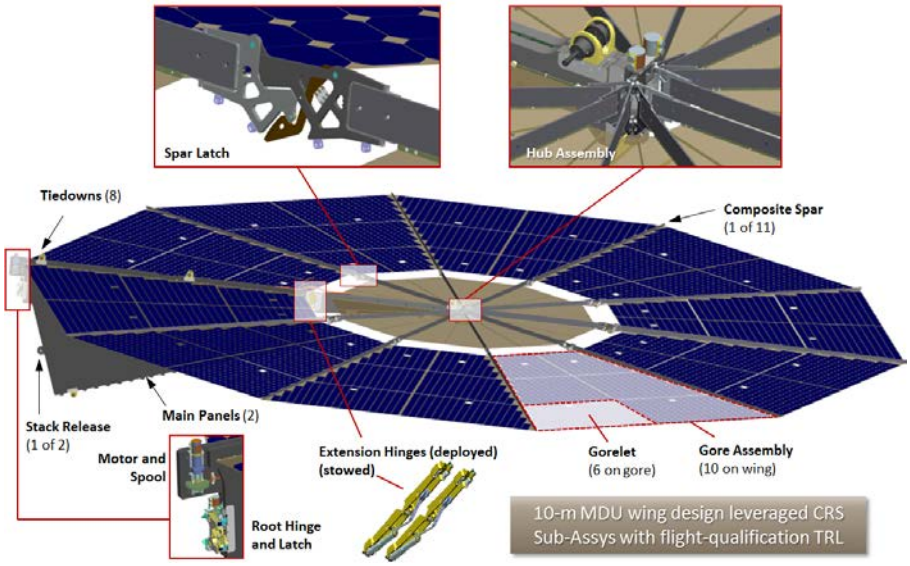

Figure 2. Key Elements of the 10-m MDU Wing, Shown Deployed.

Power wiring from each gorelet is routed over to and along the adjacent spars, through the central hub, and then toward the wing root.

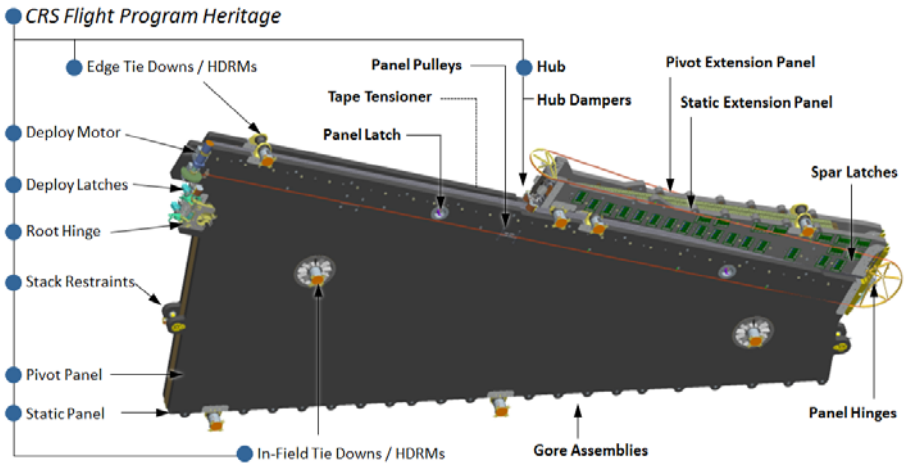

Figure 3. Key Elements of the 10-m MDU Wing, Shown Stowed.

The two adjacent spars located at the mid-plane of the wing are connected by springs to provide uniform tension in the overall blanket throughout thermal extremes and combined with external dynamic loading.

Sparlets on the gore adjacent to the panels are attached to the graphite-skin, aluminum-honeycomb core sandwich panels with a row of small and light threaded inserts.

The panels serve dual purposes, supporting the blanket (via the spars, which converge at the hub) in the deployed configuration, and acting as a protective housing for the populated gores in the stowed configuration. The deployed wing is illustrated in Fig. 2, and the stowed configuration in Fig. 3.

The deployment of the wing is accomplished in three stages: (1) *staging* away from the host spacecraft (including an offset boom if needed), (2) *extending* the folded spars and panel sub-sections, and (3) *unfurling* to achieve a tensioned and latched high-stiffness and high-strength configuration.

The sequence for the deployment of the stowed wing is initiated when the launch tie system is actuated to release the wing from the spacecraft sidewall.

A number of Hold-Down and Release Mechanisms (HDRMs) release the SAW from the stowed configuration; there are eight on the 10-m MDU. Staging of the SAW away from the spacecraft involves rotation about an axis located at the root of one of the main panels. This hinge is located on the Static Panel, so-named because it's static during deployment of the Power Assembly.

Employing this reference frame to our advantage, the static panel is the element of the SAW supported by GSE to allow end-to-end validation of wing deployment in a thermal-vac environment (without any human intervention between stages).

In the MDU test configuration, the spacecraft sidewall simulator rotates away from the static panel. The sidewall rotational inertia is matched to that of the wing to create equivalence for performance evaluation of the root hinge.

Staging is driven by redundant springs and retarded by a torsion damper. Telemetry from redundant microswitches provides indication of the completion of wing staging, which is the first part of the 3-phase deployment series.

Views from a demonstration of *staging* in the Plum Brook vacuum chamber (at ambient conditions) are shown in Fig. 4, followed by views of the *extension* phase in Fig. 5.

Extension is driven by a motor located at the root of the static panel. This same motor powers the wing to full deployment in the final phase, *unfurling*, shown in Fig. 6.

To accomplish extension with the same motor as unfurling, a static lanyard reel was added to the portion of the static panel which gets extended with MegaFlex (vs. UltraFlex). Because the pivot panel is still constrained to the static panel during extension (by a pair of small Frangibolt HDRMs), the tension in the motor-driven

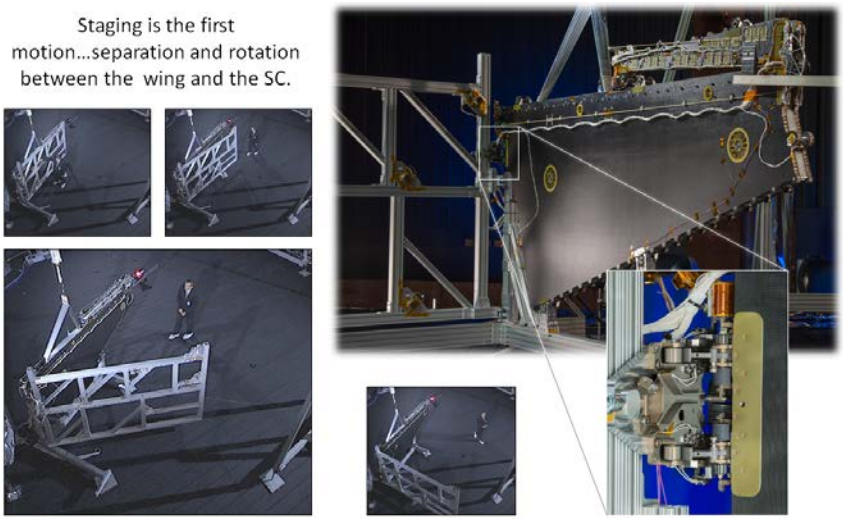

Figure 4. Deployment Sequence Phase 1 - *Staging*

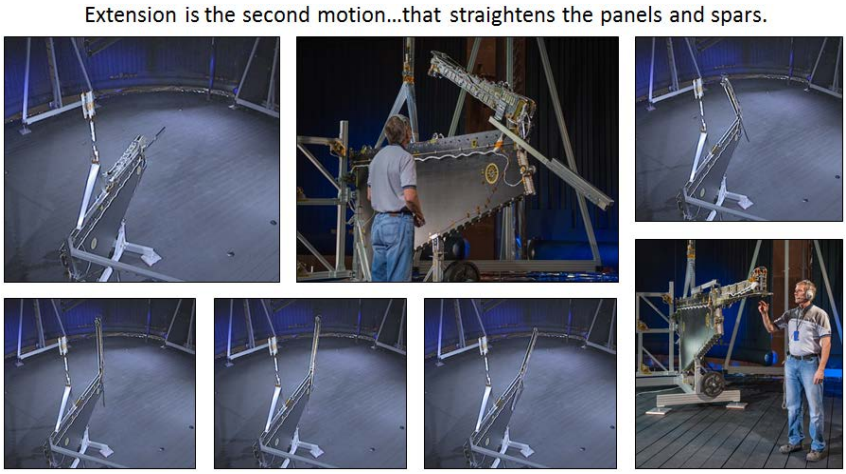

Figure 5. Deployment Sequence Phase 2 - *Extension*

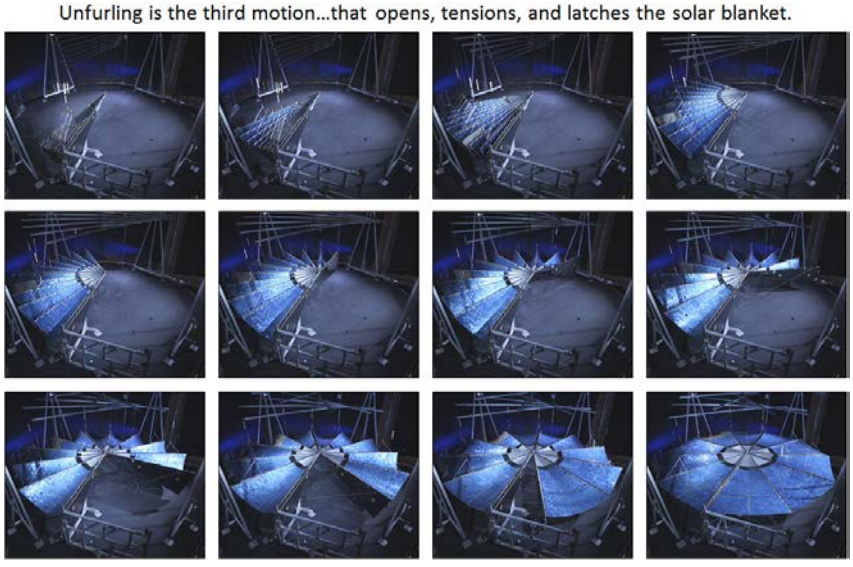

Figure 6. Deployment Sequence Phase 3 - *Unfurling*

lanyard creates a moment which rotates the extension panels with the reel, carrying-along the pivot extension panel and folded spars. For ground testing, this assemblage is counterbalanced for gravity effects by a (non-flight) beam and mass (viewable in Fig. 5).

Near the completion of rotation, springs drive the two extension panels into position to latch, which is indicated by switch telemetry and the motor is shut off. Each of the spar joints latch simultaneously with the latching of the two extension panel hinges.

Next, to begin the unfurling phase, the two remaining HDRMs between panels are released to allow the stack of gores to be unfurled. The deployment of the blanket is driven by restarting the motor, and the lanyard continues to wind up on a spool. At the end of unfurling, latches are captured in three locations along and between the panels to establish uniform gore tension, and telemetry from several (redundant) microswitches confirms latching to complete the deployment.

End-to-end validation of the deployment of the MDU SAW was achieved with the wing deploying in vacuum at hot and cold extremes of ±60 °C. Additionally, the wing was exercised with more than 30 total deployments to demonstrate the repeatability, reliability, and lifespan of the overall system, and particularly the new mechanisms developed for MegaFlex.

B. Development Background

The philosophy driving the MegaFlex design development program plan was to focus efforts on those aspects most affected by scaling up to the sizes envisioned for use in future SEP missions. MegaFlex/UltraFlex maintains much of the same basic design architecture and deployment mechanization whether it might be for a large 350-kW (2-wing) array or for a much smaller 3.5-kW application like the Commercial Resupply Services (CRS) Cygnus vehicle. However, the details of how larger wings are to be manufactured and assembled were evolved to improve production efficiency, resulting in new designs for the gores and their connection to the spars. Of course, the key feature that distinguishes MegaFlex from UltraFlex – the secondary folding capability – was the focus of intensive efforts to develop and thoroughly validate to increase the technology readiness level (TRL) of the overall system.

When the MDU design activity started, OAG (ATK at that time) was qualification testing the first flight wings for the Cygnus CRS vehicles for Orbital Sciences. This production program has completed building, testing, and delivering the first of 10 identical flight wings, and has begun a second phase with 16 additional wings.

Based on preliminary analysis, all mechanism designs for the 3.7-m-diameter CRS wing were expected to be suitable for use on the 10-m-diameter MegaFlex wing. The CRS wing is extremely strong and able to withstand the equivalent of a 5.5-g loading, protecting against the possibility of plume loading from other visiting vehicles while CRS is docked at the ISS. In general, the mechanisms from the smaller 3.7-m CRS wing design satisfied the requirements for the 10-m wing due to the extreme strength afforded by the qualified CRS wing design. With significant re-use of the CRS-based mechanisms, the MDU design activity was able to focus more intently on optimizing the design of the gores, as well as the design of the MegaFlex-specific spar and panel extension mechanisms.

All subassemblies are depicted and labeled in Fig. 2 (deployed) and Fig. 3 (stowed). The latter figure is color-coded to indicate the subassemblies adopted from CRS without significant modification.

The mechanisms added to achieve the distinctive MegaFlex extension were demonstrated at the outset of the program with a dedicated test bed: the FSP, views of which are depicted in Fig. 7.

This full-scale demonstration hardware incorporated all the components related to achieving the secondary fold distinct to MegaFlex: Panel Hinges (2 ea.), Spar Hinges (10 ea.), and Deployment Drive System (tape routing and guides).

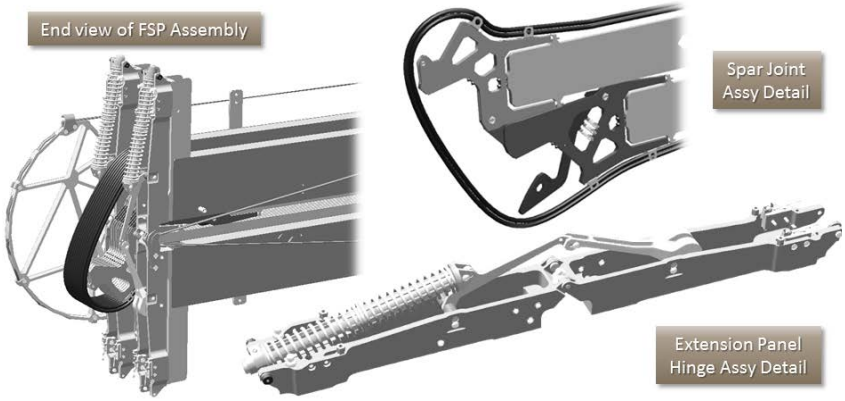

Figure 7. Folding Spar Pathfinder (FSP) Elements

A detailed view of an actual Latching Spar Hinge Joint is shown in Fig. 8 on the next page.

Figure 8. Folding and Latching Spar Joint Assembly Hardware

The PV blanket design was reconsidered in almost every aspect for MegaFlex, primarily for manufacturability and mass, with improvements including: how the gore substrates interface with the spars, the scrim material itself, the laydown (bonding) of cells to the scrim, the arrangement of foam to cushion the cells in the stowed blanket stack, and electrical harnessing to facilitate modularity and assembly.

A number of engineering test coupons were built and tested to investigate new designs, including: scrim (bending strength, flexibility and toughness), gorelet coupons with bonded sparlets (strips bonded to scrim edges to allow modular assembly), cell laydown on scrim, and a complete blanket stack-up coupon to evaluate stowed height and stiffness.

Lastly, given the scale of potential MegaFlex wings, the relation between design configuration and assembly options was reconsidered relative to heritage UltraFlex processes. Assembly labor and complexity was significantly reduced by incorporating features for modularity and self-tooling features, and by limiting overall dimensions of components such as gores to a very manageable size, regardless of wing size, for ease of handling and integration. With 1-piece spars and sparlets on the gorelet edges, platform assembly and deployment checkout can now be performed in-parallel with Gorelet production, as diagramed in Fig. 9.

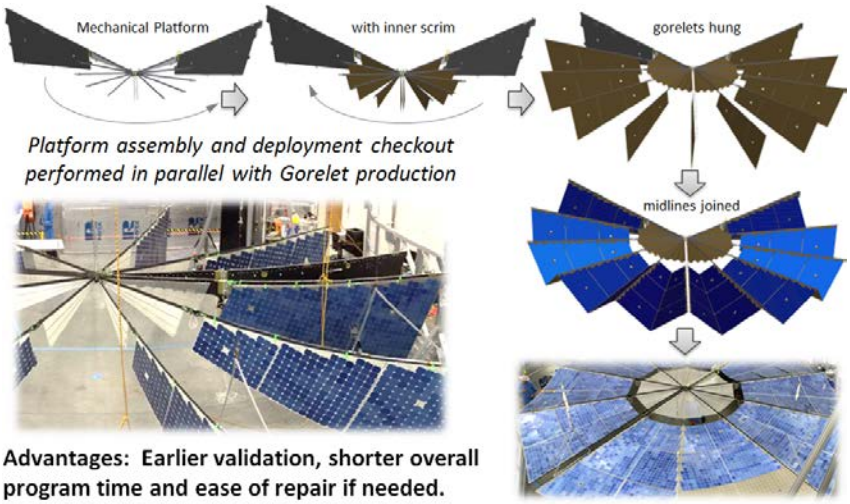

Figure 9. Parallel Flow in MegaFlex Platform and Power Assembly

This approach provides several significant advantages, such as earlier mechanical and electrical platform functional validation prior to gore integration, shorter overall program time by allowing fab-rication of the platform and the power assemblies in parallel), and ease of repair of PV elements, if needed, by the ability to quickly remove a gorelet.

Even the very largest (e.g. a 30-m) MegaFlex wing would be produced with the same modular gorelet approach demonstrated on the 10-m wing.

C. Trade Studies

From the beginning of the program effort, an evaluation of the *entire* wing system was pursued with the goal of developing a MegaFlex design that best balances physical performance metrics (e.g. W/kg, strength, stiffness, W/m^3, high voltage) with feasibility (affordable $/W, manufacturability, scalability with minimal NRE, low risk with high TRL, and reliability).

The result was a MegaFlex solar array design that exceeded the high physical performance goals specified by NASA, *with* modularity and manufacturing efficiency on-par with a state-of-the-practice planar array. Extensive tooling and handling GSE used on CRS UltraFlex were practically eliminated from the MegaFlex design by making use of self-tooling bonded assemblies. Wherever possible, manufacturing tolerances were accepted in lieu of assembly adjustability or shimming. Taken together, these efforts provided significant cost savings to the MDU, but most importantly make future MegaFlex systems cost-competitive, including the very large systems envisioned to one day support human missions to deep space.

Trade studies were performed on numerous key subsystems, critical examples of which are discussed in subsections below. The goals were to optimize the following key objectives, among a host of other design specific requirements:

- Specific power (W/kg)
- Packing efficiency (W/m^3)
- High voltage (plasma environment)
- Reliability and Robustness
- Affordability ($/Watt)
- Extensibility (scalability)

Spacecraft Tiedowns: Very early in the program, a simplified FEM of the stowed MegaFlex wing was generated to investigate the effect of Hold Down and Release Mechanism (HDRM) quantity and placement on the wing, and an optimization was performed. First, the panels were sized to provide the minimum required deployed stiffness (with margin). This panel size happened to be very close to the CRS panel core and facesheet thickness design, and this thickness was also acceptable for optimization for stowed W/m^3, a key metric for large solar arrays and a metric tracked by this program. Then, for the chosen panel configuration, HDRM placement was evaluated to minimize the number of locations in which the devices would pass through cutouts in the panels and gores. Some of the HDRMs were located at the edge of the panel in order to ensure that cup-cone engagement along the sparlets is maintained during launch, thereby eliminating the dependence on blanket pressure to achieve in-plane restraint of the blanket stack. A "low blanket pressure" design was a notable improvement over the CRS design, which relies on relatively high foam preload to prevent in-plane movement of the blanket mass. Eight HDRMs for launch constraint were used on the MDU, distributed as can be seen in Fig. 3.

Gore Count: Several considerations go into selecting the optimum gore count for a given wing diameter. Using a detailed parametric system model, OAG has performed optimization studies to determine guidelines for gore count vs. wing size. In general, the addition of gores adds additional spars and mechanism to the wing, but reduces panel size and HDRM quantity. For a given wing size, specific power (W/kg) can be optimized while also limiting gorelet proportions to a manageable size for manufacturing and minimizing the stowed envelope (W/m^3). For larger wings the gore count increases. The MDU scale of ~10 m (9.7 m, tip-to-tip) was found to fall within the optimal size range for a 10-gore wing, allowing use of the qualified CRS hub design. One may refer to Section XII for more information on scalability and extensibility, including a plot of wing mass vs. diameter, and Fig. 16 depicts the preferred gore counts for a wide range of wing sizes.

Spar Sizing: As in other trades, a preference was to first determine if we could maintain the CRS dimensions as the starting point for the MegaFlex design. It was determined that the robust sizing for the much smaller CRS wing was actually well suited to the 10-m MegaFlex wing design goals of 0.1 Hz for the first mode and 0.1-g strength. The maximum height of the tapered CRS spar was maintained constant across the first third of the radius (the unpopulated gore zone in the center) and then tapered to a ½-in. height at the tip. Due to the additions of sparlets at the edges of the gorelets, the spars could be constructed as a single monolithic laminate, as opposed to the dual-spar half "scrim sandwich" employed by previous UltraFlex designs where the spar halves are bonded together with the scrim secured between. This change improves manufacturability and also buckling strength, as the spar torsional stiffness is increased significantly, when compared to the sandwiched spar construction where two spar halves are bonded together with silicone bonding agents. The GJ of the spar, which is fundamental to the lateral buckling strength, increases by 3-4 times when using a monolithic spar versus the previous UltraFlex-heritage 2-part spar construction. The increase in structural performance offsets the mass addition of the sparlets, which are key to improved manufacturability, integration, and ease of repairs.

D. Detailed Design Modeling

The MDU mechanical design was performed using PTC Creo, providing 3D parametric CAD along with the ability to perform piece-part finite element analysis (FEA) and system kinematic simulation. Key design analyses performed using Creo included (but were not limited to) Mass Estimation Analysis and Correlation, Mass Properties Analysis (CG and MOI), and Deployment Simulation and Control.

The wing hardware validated the parametric MegaFlex mass model by correlating very well to the predicted 10-m wing mass. The MDU demonstrated compliance to the program mass requirement, with performance that exceeded 100 W/kg at the end of the (modeled) mission life, when the cells have accumulated a very high radiation dose, while simultaneously meeting the challenging strength and stiffness requirements.

Other design criteria focused on over the course of the program included analyses for: Magnetic Moment, EEE Parts Radiation, AO Degradation, Reliability and evaluations of Parts, and Materials and Processes for flight application. Analyses of stiffness (stowed and deployed frequency), strength (launch and on orbit), and thermal extremes are reviewed briefly in the following section.

III. Analytical Modeling

High-fidelity analyses were performed to evaluate the stowed and deployed mechanical and thermal behaviors of the wing. The FEA models developed by OAG were translated into NASTRAN for parallel evaluation by NASA.

A. Stowed Modeling

The stowed system behavior and the structural capability with respect to the defined launch requirements were investigated with models that were evolved and refined over the course of the program as the design developed and as test data on components and subassemblies became available. The modeling was employed to support and guide the design and to predict behaviors such as stiffness, modes shapes, frequency, and stress for the acoustic and random vibration environments of launch.

Verification of the modeling and the robustness of the hardware were demonstrated by testing to acoustic levels enveloping EELV environments. To validate survival to the random environment, the acoustic input was increased until accelerometers at key points responded with equal or higher RMS deflection than forecast by the FEA model. The lowest mode predicted for the stowed wing, with refinements to reflect the flight design conditions, was 28 Hz, meeting the requirement of 25 Hz minimum.

B. Deployed Modeling

The deployed behavior and capability to perform against the defined structural requirements for both in-flight (0.1-g max) and 1-g environments were considered, supported where needed by detailed component modeling using FEA, Mathcad, and Excel computations. The deployed FEA model was studied using nonlinear large deflection analyses to arrive at accurate gore tension and catenary deflections. The deflections and stiffness matrices from the nonlinear analysis were then used in modal analyses which provided frequency predictions, which ended up being within 3.5%, on average, of the first three frequencies as measured in vacuum at Plum Brook. Ground support equipment present in the offloaded (1-g) model, but not in the zero g model, included the springs and cabling associated for supporting the spars. The stiffness of these elements was individually measured and modeled. After extrapolation of the validated 1-g model to 0-g conditions, the lowest mode in flight was predicted at 0.27 Hz, which was well above the requirement of 0.1 Hz.

C. Thermal Modeling

Analyses using Thermal Desktop were performed to determine the MegaFlex temperature extremes for the baseline mission and, along with solar blanket coupon testing, to show that all components are suitable for the predicted thermal extremes with margins. Thermal analysis was used to determine the structural temperatures and gradients for use in wing Thermal Distortion and Solar Blanket Planarity Analyses. The thermal results were also used as input for solar cell operating temperatures in the power production analysis.

Temperatures were mapped from the Thermal Desktop model into ANSYS to evaluate combined stresses from thermal and on-orbit structural loading and to evaluate margins. The effect of temperature on blanket tension and system modes was also evaluated, to assure the required minimum frequency was exceeded with the blanket (and tensioning mechanism) at the limits of travel.

IV. Power Generation

A. Power Analysis

MegaFlex can generate electrical power using any type of space-grade solar cell. For this program the focus was on packaging the following space cell products for use in the high-voltage, dense plasma, SEP environment: Spectrolab XTJ, SolAero ZTJ, and SolAero IMM4J (Inverted Metamorphic Multi-junction). These cells were chosen because they include the present best state-of-the-practice space-mission solar cells (XTJ and ZTJ), as well as a leading next-generation developmental cell (IMM4J).

All NASA specifications and industry guidelines for power estimation were implemented, including analysis for the specified baseline mission consisting of a spiral orbit from LEO (400 km) to GEO; use of the specified cell electrical performance parameters, temperature coefficients, and radiation degradation data; the radiation environment; and the inclusion of a 2% MMOD end-of-life (EOL) loss factor. It was shown that power loss due to Hall Thruster plume sputtering is zero, due to the round MegaFlex wing being located out of the energetic portion of the plume, so no power loss factor is needed for sputtering. The harness resistance was calculated from the actual wire gauge and lengths used on the wing.

Radiation degradation was calculated using the JPL equivalent 1-MeV-electron method from the Relative Damage Coefficients (RDCs) for electrons and protons of differing energies provided by the cell manufacturers for the different cell technologies.

It should be noted that even with heavy shielding, the baseline mission (330-day LEO to GEO spiral-out transfer orbit) has very high radiation dose levels which, in less than a year, accumulate to more than four times the radiation dose absorbed in a 15-year GEO application.

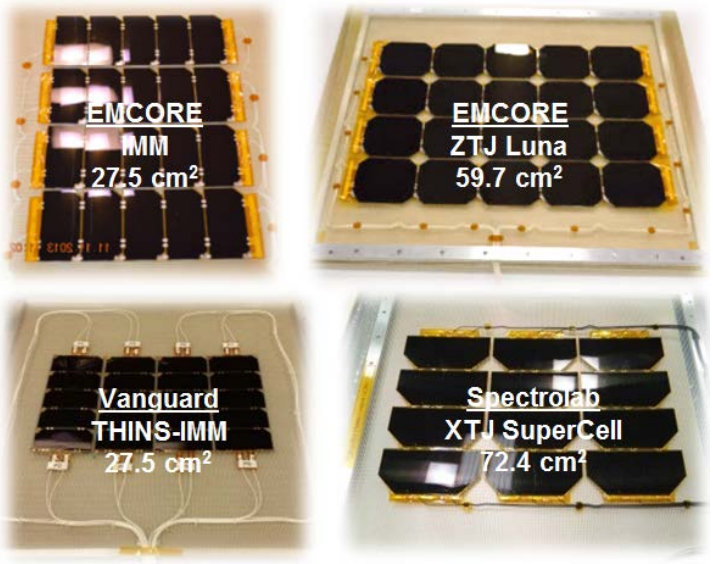

Figure 10. PV Coupons for Plasma and Thermal Tests

B. Photovoltaic Coupons

PV assemblies were prepared to OAG specifications by EMCORE (now SolAreo Technologies Corporation), Spectrolab (a subsidiary of Boeing), and Vanguard Space Technologies, in order to demonstrate power production capability and stability against the uncommon voltage, thermal cycling, and ESD requirements of the SEP Tug application. Each coupon measured approximately 0.5-m by 0.5-m and consisted of one or more strings of solar cells bonded to MegaFlex fabric mesh held in an aluminum support frame.

Plasma tolerant features were incorporated on all coupons so that they could operate at high voltage (300 V) and in dense plasma (10^8/cm^3). On each coupon the plasma tolerant features were designed and implemented uniquely by the vendors. Images of the four test coupons are shown in Fig. 10.

The PV coupons underwent initial high voltage plasma testing at JPL, then thermal cycle testing at OAG, and then plasma testing again, to investigate suitability for application to a SEP spacecraft in any orbit. The thermal cycling was grouped into representative LEO, MEO, and GEO temperature segments, with the LEO segment occurring first and the GEO segment occurring last, consistent with the baseline mission. Two thousand total cycles were performed, with temperature limits as wide as -170 °C to +120 °C. After cycling, the coupons underwent visual and electrically inspections, LAPSS testing of the power output of each string, and 1,000-V hi-pot testing over the entire electrically-active area to verify plasma isolation.

In the initial rounds of plasma testing, all coupons passed and operated with a 600 V steady state positive bias with minimal current leakage. No trigger arcs or sustained arcs were observed on any of the coupons. These tests demonstrate 100% margin against the NASA target for 300-V operations for direct-drive SEP missions.[18]

With all coupons, negative voltage bias plasma arcing was also successfully performed at -600 V with a 200-V bias between strings for 90 minutes.

After 2000 thermal cycles the Spectrolab-packaged coupon was tested again and passed

Table 1. Testing Performed on MegaFlex SEP PV Coupons

Test	Test Condition	Coupon(s)	Key Testing Result	Met Req't
High Voltage Plasma (Positive Bias)	· +600 V bias to SEP plasma · Plasma density = 1e8/cm^3	All	· Very low current leakage · I_{leak} < 0.1% string I_{sc}, all coupons · No measurable power degradation	Yes
High Voltage Plasma (Negative Bias)	· -600 V bias to SEP plasma · 200 V string to string · Plasma density = 1e8/cm^3	All	· No damaging trigger arcs · No sustained arcs · No measurable power degradation	Yes
LEO, MEO, GEO Thermal Cycling	· 667 cycle: -133°C to 120°C · 667 cycle: -154°C to 80°C · 667 cycle: -171°C to 76°C	Spectrolab XTJ EMCORE ZTJ EMCORE IMM	· Maximum power degradation of all strings less than 2%	Yes
Post Thermal Cycle High Voltage Plasma (Positive Bias)	· + 600V bias to SEP plasma · Plasma density = 1e8/cm^3	Spectrolab XTJ SuperCell = 72.4 cm^2 (Others not tested)	· Very low current leakage · I_{leak} < 0.1% string I_{sc}, all strings · No measurable power degradation	Yes
1000 Hr Endurance Test, High V Plasma (Positive Bias)	· 1000 hours · + 600 V bias to SEP plasma · Plasma density = 1e8/cm^3	EMCORE ZTJ Luna = 59.7 cm^2 (Others not tested)		Yes
High Efficiency (Integrated Blanket)	· 1 AMO Illumination · 28°C Temperature	EMCORE IMM STD = 27.5 cm^2	· Best 5-Cell String = 32.6% · Three 5-Cell Strings = 32% or better	Yes

all aspects of the positive bias current leakage test as well. Measured current leakage was compared to the nominal string current and the losses were negligible.

Additional tests were performed successfully as shown in the summary of the PV Coupon testing is shown in Table 1. The successful completion of the plasma and thermal cycle testing of the various blanket technologies of SolAreo – packaging of both ZTJ & IMM – and of Spectrolab (XTJ) cells to be promising candidates for the challenging conditions imposed by SEP missions.

C. Power Management and Distribution

A dedicated Power Management and Distribution (PMAD) coupon was designed and fabricated with flight representative hardware to demonstrate that all electrical elements for connecting PV strings to the bus would be capable of withstanding voltages of at least 300 V in the plasma environment. The coupon consisted of three circuits, each with three single string wires ganged via diode boards. Circuit wires were connectorized thru a circular connector as planned for the spacecraft interface. Verifications were performed before and after thermal cycling. No change in circuit performance was evident after all testing was completed.

V. Wing Performance

The performance requirements specified for this program were exceptionally demanding and called for performance that significantly exceeds the current state-of-the-art for large (high-power) deployable solar arrays. The key success criteria metrics (level 1 program requirements) were:

- Greater than 100 W/kg EOL power to mass ratio with 0.1-Hz frequency and 0.1-g strength (deployed).

OAG worked closely with NASA on broadening and tailoring the requirement set for the baseline SEP mission. Forty-six system-level requirements in all were imposed upon the MegaFlex design. The driving requirements of the baseline LEO-to-GEO Tug mission are extremely aggressive compared to a typical 15-year mission in GEO, as can be seem in detail in Table 2.

The combination of these driving requirements presents a greater challenge than solar array technology has ever been asked to meet before. It was shown that the 10-m MegaFlex wing, configured with 29%-efficient XTJ or ZTJ solar cells, exceeded all requirements.

Table 2. Comparison of Driving Requirements for Baseline SEP Tug Mission vs. Typical GEO Mission

Key Parameters	SEP-SAS Program Req'ts Met by MegaFlex	Key Requirements of SEP-SAS Program	Typ. Big GEO Performance	SEP Requirement vs Typical Large GEO
Array Power Level (BOL)	> 30 kW with XTJ or ZTJ (scalable to ≥ 250 kW)	This huge power range and beyond can be met with scaled MegaFlex wings (2)	15 kW	**~2X (to > 15X) Power** (and Area) **Scaling**
Mass Efficiency	> 100 W/kg EOL	Includes all mechanism, structure and power transfer up to & including all the stowed interfaces with the spacecraft.	60 W/kg	**~2X Lighter** (per Watt)
Packing Efficiency	> 40 kW/m^3 EOL		10 kW/m^3	**~4X More Compact** (per Watt)
Deployed Strength	> 0.1 g (0.2 g goal)	Deployed Strength and Stiffness requirements drive structural mass for MegaFlex and any large solar array	0.005 g	**~ 20X Stronger**
Deployed Frequency	> 0.1 Hz (0.05 Hz for 250 kW)		> 0.05 Hz	**~ 4X Stiffer** (4X Stiffness -> 2X Freq.)
Radiation in Mission	330 Day LEO to GEO Transfer Orbit	Very high radiation (2e15 1MeV e$^-$/cm^2) even with significant cell shielding, so more area is needed to begin with.	5e14 1MeV	**~4X on Radiation Degradation Potential**
Operating Voltage	> 160 V EOL (300 V goal)	Encapsulation and other treatments are needed for operating in dense plasma (thruster) or GEO ESD environment	32 V to 105 V	**~1.5X (to 3X) Higher Voltage**
Stowed Frequency	> 25 Hz	SEP wings will be challenged to perform to the same requirements at smaller wings while scaling up to 10x larger. More tiedown points and/or larger SC interface fittings will be needed for very high power wings, even with high W/kg.	> 25 Hz	Typical requirements, met by 10-m MegaFlex wing. Requirements for wings 10x larger (and 10x more total mass) will not be like what has ever been attempted before…
Stowed Strength	20 g in Each Axis		20 g	

The performance of the 10-m wing against the top level requirements, which is discussed in the subsections that follow, is summarized in Table 3. Larger, higher-power wings were also studied to validate that these metrics can be reached with wings as much as 10 times larger in deployed area. The extensibility of the technology, and the performance versus diameter, is presented in Section VII.

Table 3. Summary of MegaFlex Testing for Key Requirements

Test	Requirement	Key Testing Result	Analytical Correlation	Met Req't
Mass	> 100 W kg EOL	W/kg verified. Measured mass within 1% of analytical model.	Yes	Yes
Dimensional	> 40 kW/m^3	Stowed volume (W/m^3) verified	Yes	Yes
Ambient Deployment	30 stow and deploy cycles	Wing deployed > 30 times validating reliability & repeatability	Yes	Yes
Acoustic Vibration	145.2 dB OASPL	Nominal deployment, visual inspection & electrical performance after launch vibration testing	Yes	Yes
Random Vibration	11.1 g_{rms} 0.1 g^2/Hz peak 153 dB OASPL		Yes	Yes
Cold Deployment	> +60°C <10^{-4} Torr	Successful deployment and latching with greater than 2x torque margin	Yes	Yes
Hot Deployment	< -60°C <10^{-4} Torr		Yes	Yes
Deployed Frequency	> 0.1 Hz	f_n > 0.25 Hz. Exceeds goal of 0.1 Hz.	Yes	Yes
Deployed Strength	> 0.1 g	> 0.12 g demonstrated	Yes	Yes
Electrical Inspection	100% Reliability	Verify pre & post each environment: · Cell circuit current /voltage & isolation · Release & motor isolation & continuity	Yes	Yes

A. Power at EOL

Detailed power analyses, for BOL to EOL conditions, for the various photovoltaic choices were performed. The size of the MDU provides enough area for solar cells to surpass the requirement for power production at BOL. The array (2-wing) power is in excess of 36 kW using XTJ (or ZTJ) and is nearly 41 kW with IMM solar cells. Incorporation of advanced IMM cells improves beginning-of-life (BOL) power.

For the baseline spiral-out Tug mission, an optimization study was performed to determine the optimum coverglass thickness to achieve max system EOL specific power (W/kg) performance for each solar cell technology. The resulting radiation degradation reduces the power from BOL to EOL by 28% for XTJ/ZTJ (with 6-mil glass) and 31% for IMM (with 8-mil glass). The radiation degradation for IMM is based on limited preliminary radiation data sets which may be updated as IMM moves into production and more data is collected.

B. Specific Power

To determine specific power, detailed MDU-specific mass correlation (validated by weight measurements of the MDU hardware) and power analyses were performed, as described above. The MDU wing included mass simulators sized to the equivalent weight of state-of-the-practice solar cells with appropriate coverglass. The theoretical PV-populated wing was configured with a (1-cell per wafer) cell layout and a specific glassing thickness to achieve near the optimum EOL W/kg performance for the baseline mission.

The predicted specific power for the 10-m MDU equipped with XTJ cells, protected by 6 mil coverglass, is over 100 W/kg at EOL. This prediction assumes cell degradation at EOL consistent with the baseline mission. When using IMM cells with 8-mil coverglass, the predicted W/kg performance at EOL improves. The accuracy of wing mass predictions used to develop specific power figures was demonstrated with the MDU; the measured mass of the MDU was within 1% of the prediction based on the mass model.

The specific power calculations assume an operating voltage of 160 V EOL, although the PV coupons were tested to demonstrate >300 V capability. The deployed frequency and specific power performance metrics were also developed assuming the same harness mass. Although lower operating voltages require more harness runs (due to more strings for the same total power), the MDU was built with harnessing appropriate for a 160 V system rather than a 300 V system. Building with the heavier harness used on a 160V system introduced conservatism in mass as well as parasitic losses that must be overcome during deployment due to the increased harnessing. But the specific power performance would increase only slightly for a 300-V design – for a wing of this size – due to a reduction in the required harnessing. The mass advantage for employing the higher voltage would accrue to ~5% on a 100 kW array, and more on even larger wings.

C. Deployed Frequency

Typically high power solar array wings for GEO missions are designed to obtain a first mode of 0.05 Hz. The MegaFlex wing was demonstrated (in vacuum) to have a deployed natural frequency greater than the required

0.1 Hz, which requires 4x more stiffness. Stiffness tests were performed at the subsystem level on the extension hinge elements. Results were within 10% of the FEM predictions. This requirement was verified by both analysis and testing of the MDU. The measured 1st mode, extrapolated to 0-g, was 0.26 Hz, which provided a significant stiffness margin above the requirement. The strength requirement drove the structural sizing (e.g. spar cross section), and the circular configuration efficiently utilizes the material to provide a very high deployed stiffness.

D. Deployed Strength

Typical high power solar arrays for GEO missions are required to withstand accelerations up to 0.005 g while deployed. The deployed MegaFlex wing must withstand accelerations as high as 0.1 g, which is 20 times higher than a typical large array. Strength testing was performed by allowing spar tip deflections *out-of-plane* (in both directions) to an equivalent g-level of 0.1 g with a 1.2x test factor. This test loaded the spars, hub, extension panels, and panel hinges. The MDU was subjected to the on-orbit hub in-plane *lateral* g-level of 0.1 g with a 1.2 factor of safety in both directions, thereby successfully validating the hub mechanism, extension panels, and hinges.

E. Stowed Strength and Frequency

The static acceleration requirement for the stowed wing was 20 g in each axis. This requirement was confirmed by analysis that demonstrated positive margins of safety for the MDU. In addition, the wing was subjected to the dynamics of the launch environment, to levels which enveloped the maximum predicted acoustic qualification environment of 145 dB OASPL. Following this initial acoustic test, the levels were increased until accelerometer responses matched analytical predictions for deflections in response to the random vibration qualification requirements, resulting in an OASPL of 153 dB.

The stowed frequency of the MegaFlex design was predicted as 28.4 Hz, which exceeded the required 25 Hz. The response of the accelerometers in acoustic testing could not be used to precisely identify the lowest modes.

F. Stowed Volume

The predicted power packing efficiency of the MDU exceeded the requirement of 40 kW/m^3. This level of performance, which is 4 times higher than typical planar arrays, was verified via dimensional inspection of the manufactured wing convolved with BOL power analysis for XTJ/ZTJ cells. In addition to meeting this requirement, the extensibility study of the MegaFlex architecture demonstrated excellent compatibility and adaptability to various launch vehicle fairings at power levels as high as 450 kW.

VI. Test Program

The verification of the MegaFlex design, and performance against the requirements that drove the design, was intentionally weighted towards validation by test. The test program for the MegaFlex wing was constructed to follow a test-like-you-fly philosophy, both in the order and the extent of the testing. An overview of the wing test series is shown in Fig. 11.

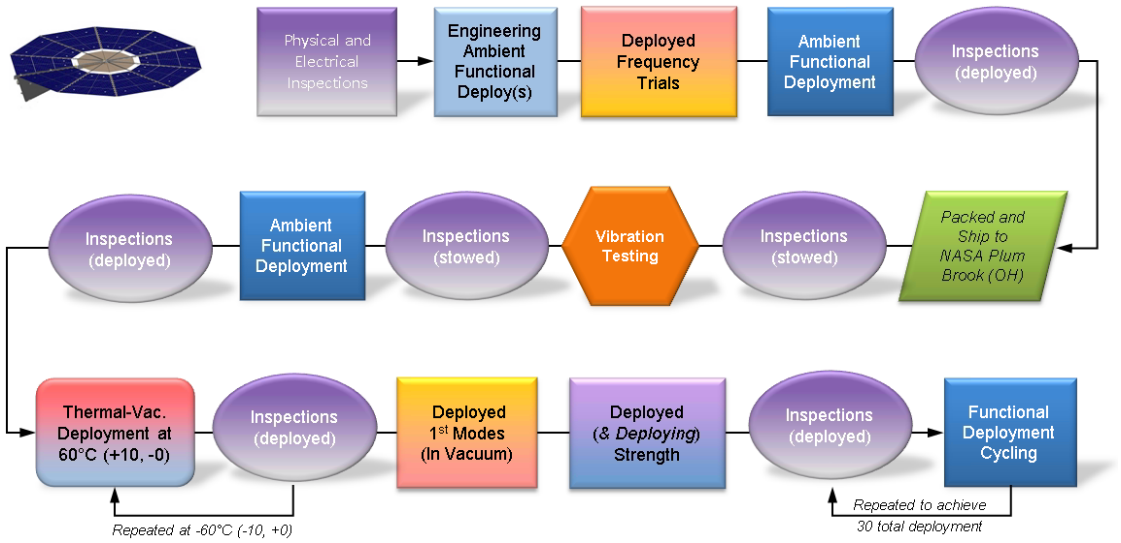

Figure 11. MegaFlex Wing-Level Test Program Flow

Leading up to the wing test series, a number of component-level tests were performed to help retire risk associated with the newest (lowest TRL) mechanisms. These mechanisms, which enable the characteristic MegaFlex extension, were demonstrated with the Folding Subsystem Pathfinder test bed. The FSP incorporated all the components related to achieving the secondary fold unique to MegaFlex: Panel Hinges (2), Spar Hinges (10), and Deployment Drive System (tape routing and guides). Other components of the wing that were tested separately included the PV coupons and PMAD hardware, which were reviewed above.

Wing-level testing began with a series of deployments and other informal engineering evaluations as the top assembly was being completed. There were some items that needed to be reworked or were left to be worked out at the wing level, such as harness routing, cable management, and deploy speed profiles.

The operation of the GSE required some adjustments to the balance of the overhead offloader, and the addition of constraints to avoid entanglement of the GSE support lines. As soon as all the hardware (wing, overhead offloader, stand, and spacecraft sidewall simulator) were performing as desired, the wing was shipped from Goleta California to the NASA GRC Plum Brook Station facility in Sandusky Ohio.

Wing testing began formally at Plum Brook in the acoustic chamber. Afterward, the wing was deployed (at room temperature) and inspected to verify the initial GSE set-up at Plum Brook, wing electrical functions, and mechanical survival after the launch environment exposure. The same series of physical and electrical inspections were performed after each environmental exposure, including the deployments at thermal extremes, and strength evaluations. Deployed strength and stiffness testing results were touched upon in Section V above. Expanded discussion of the most important tests – stowed strength (launch environmental exposure) and deployment testing (at thermal extremes) – are presented in subsections that follow.

A. Launch Dynamics

The MDU wing was exposed to acoustic levels typical of 4-m fairing launchers in the Reverberant Acoustic Test Facility (RATF). The MDU was also exposed to an even higher acoustic spectrum in order to develop response levels similar to that predicted from FEA of the wing in response to a mechanical (random) vibration environment. The wing was inspected before and after each environment, and no indication of damage was observable in any aspect of the condition of the hardware.

The RATF acoustic spectrum was able to closely meet the desired baseline environment profile, up to ~1000 Hz, but at higher frequencies excess energy from chamber reverberations was unavoidable. This energy added a significant amount of higher frequency response into the accelerometers, but induced very little additional total deflection (and thus little additional stress) into the MDU. The spectrum for the as-tested baseline acoustic (BA) environment is compared to the "random" vibration (RV) environment (and the BA target profile) in Fig. 12.

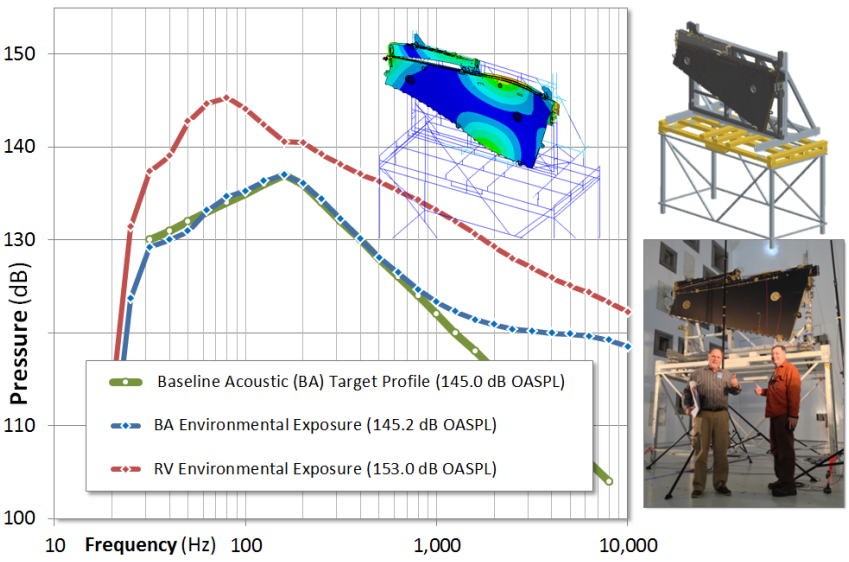

Figure 12. 10-m MegaFlex Wing Launch Vibration Testing

In aggregate, the RV environment was 8 dB above the required (baseline) acoustic profile, which means the overall sound pressure level was raised by a factor of 2.5. The levels in the RV test in some of the lower 1/3 octave bands (spanning 28–112 Hz) were intentionally driven 8 to 12 dB higher. The wing responses were largest from 50 to 130 Hz. The RV spectrum was shaped to induce RMS deflections that approximated the levels predicted by the RV FEM analysis. Most, but not all areas of the wing were exposed to the levels of stress that would be experienced in a true random vibration environment (which was not performed due to cost limitations).

Based on comparing the RMS deflections between test and FEA (from random analysis) across the overall panel, the correlations were reasonable, but using a block pressure methodology (in ANSYS) on the extension panel resulted in predictions of a much greater acceleration response than was seen in test, because the relatively small width of the extension panels results in far less pressure being applied in test than with a uniform pressure

assumption. Although the pressure levels in the 1/3-octave bands were increased until there were several areas where the margin was reduced to zero, the levels of deflection on the extension panel were still below the targets (as predicted from random vibration). There are two other effects that cause the response in the acoustic test to vary from the RV FEA predictions. The first is that the mass of the PV blanket is not as effectively coupled to the structural panels when the excitation force is via external pressure waves to the panel surfaces as it is through the excitation of a shaker table. Secondly, the fundamental (lowest) modes of the wing are not excited unless the PV and panel masses are moving together. For these reasons, one cannot as easily deduce the natural modes of the structure from acoustic response data as one can with base motion excitation.

The robustness of the design and the fidelity of the fabrication processes of the MDU wing were validated in part by virtue of having survived – without any damage – the BA and RV environmental exposures. In the post-acoustic deployment the wing performed as expected.

B. Deployment Testing

Functional evaluations were performed at several points in the Plum Brook test series to verify proper deployment at ambient and temperature extremes. All deployment testing was performed in the Space Simulation Vacuum Chamber (SSVC), at the pressure at less than 10^{-4} Torr for the hot and cold extreme temperature conditions. Deployments were performed end-to-end without intervention with controls and monitoring that represented flight-like conditions. The commands from the "spacecraft" and the recording of telemetry were performed via a LabVIEW-based computer interface system. Formal success criteria included proper release of the tiedowns, smooth wing kinematics, functioning of the limit switches, latching, and overall time duration. Verification of performance to all requirements was demonstrated.

The hot deployment was performed in vacuum with the wing and GSE hotter than 60 °C. The temperatures were controlling by the flow of heated nitrogen to the chamber walls after evacuation to below 10^{-4} Torr. Pumping down required 5–6 hours, and the wing hardware reached the dwell temperature range (60 to 70 °C) in another 5 hours. After the completion of a 20-minute dwell, the release of the HDRMs was initiated and the nitrogen flow was stopped (to avoid potential vibration of the wing stand and overhead offloader).

The cold extreme deployment, which is typically more challenging for a deployable than the hot extreme, was performed in vacuum with the wing and GSE colder than -60 °C. An overview of key telemetry alongside images of the wing at several stages of deployment is depicted in Fig. 13.

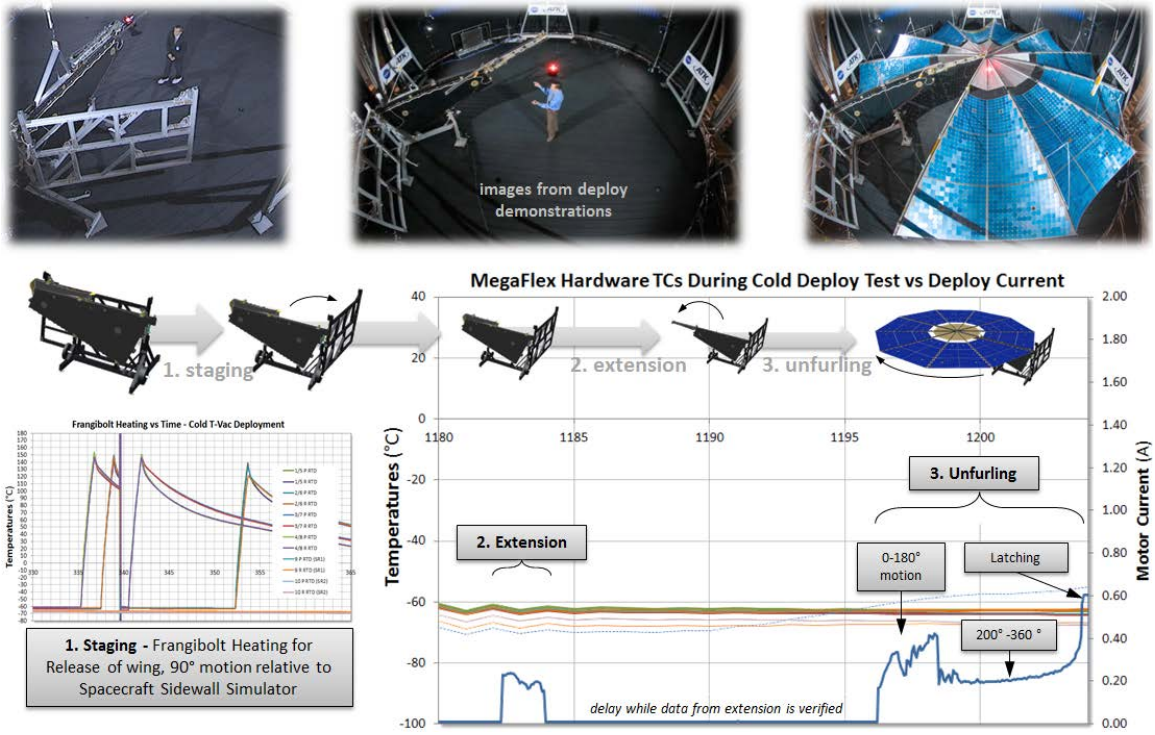

Figure 13. Deployment in Vacuum at -60 °C at the NASA-GRC Plum Brook Space Power Facility

The chamber was vented and partly cooled, which required pumping for 6 hours, followed by cooling for another 12 hours. After a dwell period below the target temperature, the eight HDRMs were heated in pairs and shut off after release (at ~140 °C), after a period of 1.5 minutes on average. The wing staged through the 90° motion in one minute and 48 seconds.

After the staging event was completed, the motor was started to tension the lanyard and drive the extension, which required 1.5 minutes to complete. The duration in the cold test was 9% slower than during the hot test, as the DC brush motor was running slightly slower due to higher parasitic losses for harness bending. A comparison of the torque traces between the cold and hot extension events is shown in the plot on the left in Fig. 14.

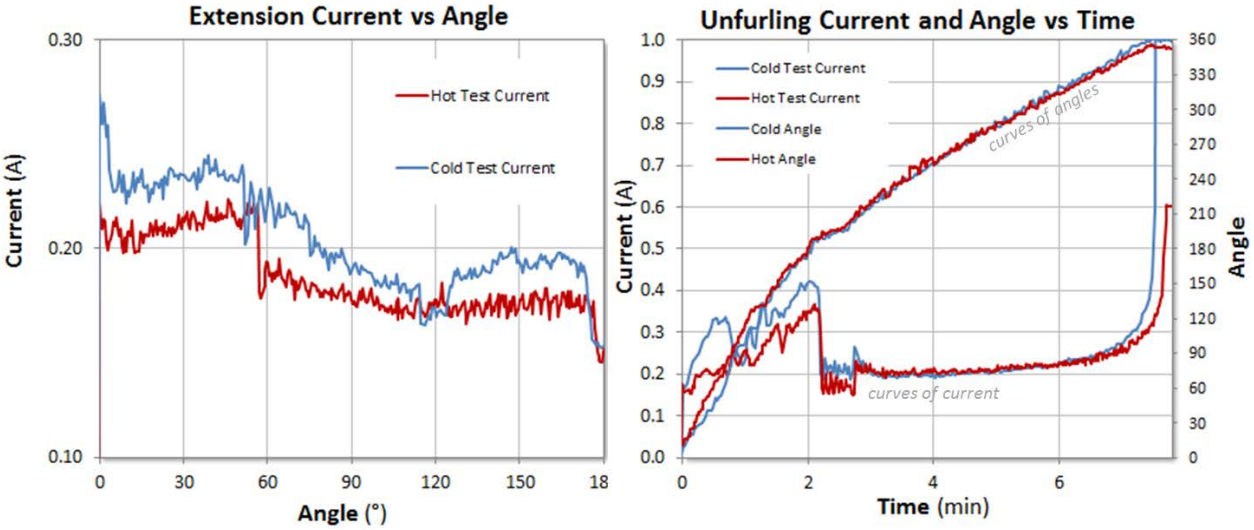

Figure 14. Comparisons of Data from Extreme Temperature Vacuum Deployments

Unfurling required a total time of 7.5 minutes to bring the pivot panel around to the latch position, which was 11 seconds faster than when hot. The motor ran slightly faster (more efficiently at cold) during the long duration running at the low torque levels required from 200° to 300°, resulting in a total time that was 2.4% faster overall. A comparison of the torque traces (motor torque is directly proportional to current) between the cold and hot unfurling events is shown in the plot on the right in Fig. 14.

As always, building high-fidelity hardware and doing repeated functional tests proved very beneficial. We were able to validate the mechanism life and flush out design, procedure, and GSE issues which are difficult to foresee. Ultimately, this resulted in validating that the mechanism design will function robustly as intended, and valuable experience was gained for a future flight test program.

On any flight program, end-to-end (test-like-you-fly) testing with a qualification or protoflight unit would be prudent. Only by testing the entire system in the highest fidelity environments achievable on the ground can the risk of failure in flight be properly mitigated. The ISS solar arrays suffered deployment failures due to incomplete testing, and required crew intervention with a potentially dangerous EVA. Autonomous deployment is a critical task, and a system must be engineered and tested under flight-like conditions to assure reliable operation[19]

VII. Scalability

Another key program task was to show extensibility to a system power level of 250 kW or greater while maintaining performance in specific power (>100 W/kg) and strength (>0.1 g) without the first mode dropping below 0.05 Hz. In order to explore the scaling performance trends, a trade space of six wing sizes was selected, ranging from the 10-m, 10-gore wing up to a 30-m, 20-gore wing.

Starting with a series of detailed power sizing spreadsheets, a metrics summary table was created, divided first into two primary cell types, and then subdivided into “Tug” and “GEO”. The Tug mission was the SEP-SAS program baseline, and the GEO cases were added to document the higher performance possible for a more typical set of requirements. A solar array in GEO runs cooler and accumulates less radiation damage over 15 years, even when shielded with much thinner (lighter) glass, versus the 300-day baseline LEO to GEO tug mission.

The extensibility tools were grounded in MDU-validated metrics and flight-proven power sizing tools, assuring the performance predictions for larger wings are valid. With the spars being critical structural components for system strength and stiffness and a significant mass fraction of the total wing, a substantial portion of the scaling exercise was dedicated to accurate spar sizing. Another important portion of the scaling effort was to develop a fully parametric CAD model, the primary purpose of which was to provide accurate mass and moment of inertia (MOI) values for wings of any size, gore count, and g-load. Additional benefits of the parametric CAD model included the creation of realistic launch packaging studies.

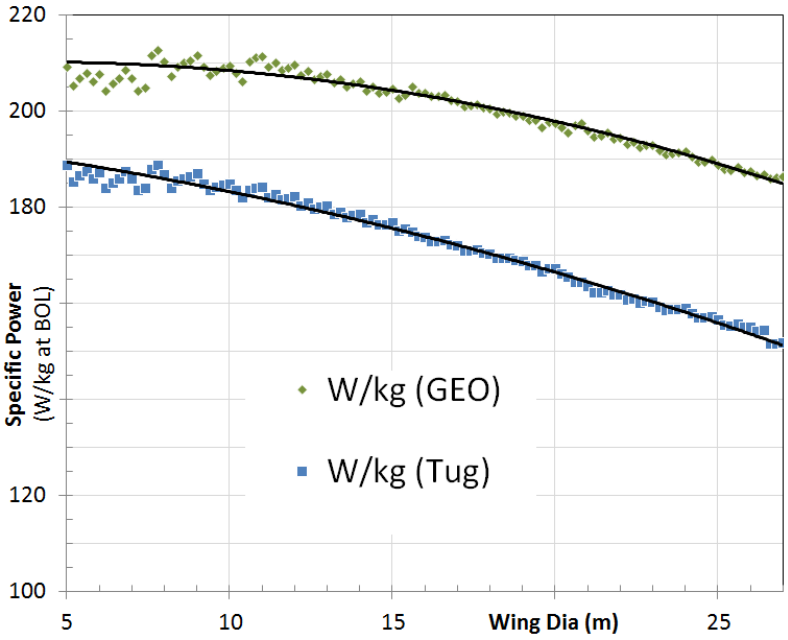

Figure 15. Specific Power vs. Wing Diameter

With the extensibility tool fully developed, performance specifications could then be created quickly for any combination of diameter, gore count, cell type, voltage, or g-load. Using the completed extensibility tool, mass and packing performance were then plotted versus wing diameter for a high number of cases. The resulting performance is presented in Fig. 15. Refer to Fig. 16 for a visual comparison of a few examples of these detailed MegaFlex systems, for wings from 15 to 30 meters in diameter, packaged in representative launch configurations.

The strength requirement, rather than the frequency, drove the wing mass over the entire trade space. The assumptions for the plotted cases were:

- State-of-the-Practice Solar Cells: 28.9% BOL
- SEP-SAS mission (Tug): 0.10 g for all sizes; 0.10 Hz at 40 kW and 0.05 Hz for > 250 kW
- Typical mission (GEO): 0.05 g for all sizes; 0.05 Hz at 40 kW and 0.025 Hz for > 250 kW

In summary, the MegaFlex system proves to be readily extensible for higher-power SEP missions extending well into the future. As wing size increases it is recognized and expected that specific power, for any system, will naturally drop off (assuming the requirements for strength and stiffness remain the same as the wing area grows). Even so, the 300-kW MegaFlex (25-m) system shows an impressive specific power, about 155 W/kg, for the specified tug mission and nearly 190 W/kg for a typical GEO application.

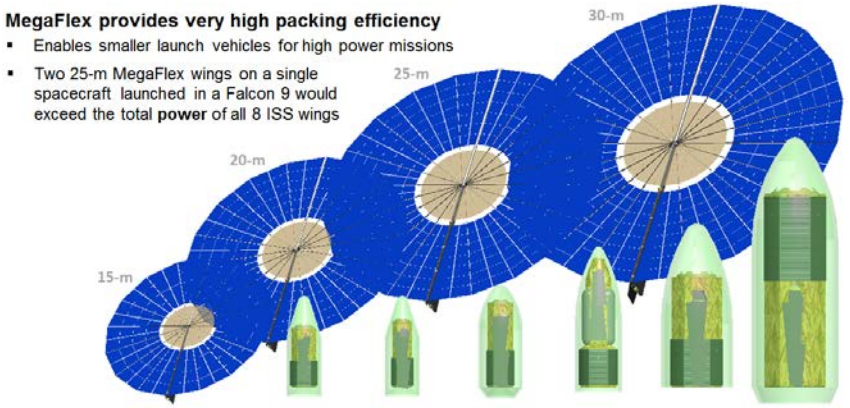

Fairing Class Fairing Diameter	Delta IV 4-m	Delta IV 4-m	Falcon 9 5.2-m	Ariane5 5.4-m	SLS PF1B 8.4-m	SLS PF2 10-m
Wing Diameter (m)	15	20	25	25	30	30
Array Power Class (kW, IMM)	105	190	300	300	450	450

Figure 16. Launch Vehicle vs. MegaFlex Power Class

Aside from the impressive metrics, it should be noted that as the target power rises and the MegaFlex wing increases in size, the total mechanism *count* does not increase, and no *new* mechanisms are introduced, just larger versions of already proven mechanical subsystems are needed.

Additionally, larger MegaFlex wings can be manufactured and tested in essentially the same end-to-end fashion as the development unit was produced, eliminating the

need for fundamental new process development. All in all, the MegaFlex wing scales naturally, consumes minimal fairing space, and performs well structurally (low mass with good stiffness and strength), thereby providing a straightforward growth path for future very high power SEP missions.

VIII. Summary

The ground demonstration and validation of MegaFlex technology has elevated the TRL in all critical areas necessary to support a low-risk flight validation mission. OAG has experience with six 2-m UltraFlex wings for NASA flight programs. Two are deployed on Mars (Phoenix, 2008) and two more be landing there in 2016 (InSight). OAG has finished a 10-wing build program of 3.7-m wings that will fly on resupply missions to the space station starting in 2015.

If the next large SEP mission requires less than 35 kW at BOL, this level of power can be accommodated with the 10-m MDU design using state-of-the-practice solar cells. If a power level as high as 90 kW is needed, this challenge can be met with just a "slightly" larger diameter – a 15-m wing system. Refer to the figure below for a hardware comparison of the Mars, CRS, and MDU wings.

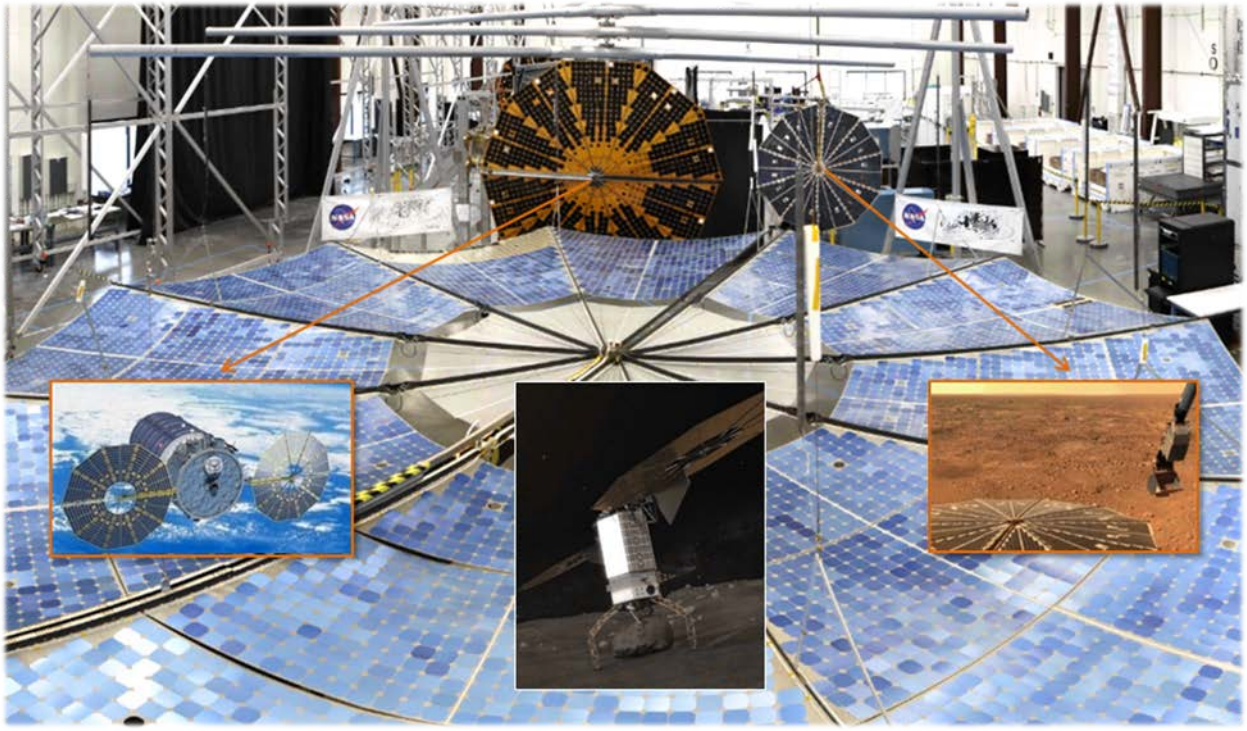

Figure 17. Comparison of 2.2-, 3.7-, and 9.7-m UltraFlex and MegaFlex Systems

Our experience and success with scaling-up the diameter by 75% (Mars to CRS) and then by 160% (CRS vs. MDU), demonstrate that a 15-m wing is a reasonable, low risk increment. That would only be an increase in diameter of 55%, which is much less than either of the two scalings previously accomplished.

Scaling the diameter by 1.5 increases the available area by the square, or 2.25. Continuing to increase the diameter yields an enormous capability for powering future missions. For example, a 25-m MegaFlex SAS with IMM solar cells would deliver over 300 kW, which is 50% more than all eight solar arrays on the space station produced at BOL. And, a 300-kW SEP spacecraft outfitted with MegaFlex wings can be lifted to orbit in launch systems available today, as depicted in Fig. 16.

Given the significant development and validation accomplished within the SEP-SAS program, design time and NRE will be significantly reduced for a flight program. If the program is schedule-driven, MegaFlex will provide a quick and smooth path to PDR, and avoiding the impact of a protracted NRE phase will also save program funding.

The MegaFlex system offers uniquely high-performance, high-TRL solar array technology, backed by OAG's 100% flight success record across 4 decades, with more than 40 wing deployments on-orbit in the past 4 years alone, to support whatever the future may hold for exploration beyond earth orbit that SEP technology will soon enable.

Acknowledgments

The SEP-SAS MegaFlex program was performed under contract number NNC12CA43C from the NASA Glenn Research Center. The authors would like to extend thanks to all the people who contributed to this effort, including the Solar Electric Power Element Manager at NASA Glenn Research Center, Carolyn Mercer, and the technical lead, Tom Kerslake, and all the valuable project support provided by the many who participated at Glenn and Langley, and especially Plum Brook Station. In addition, we give thanks to the partnership and participation provided by NASA JPL, Ball, AMA, Spectrolab, Emcore, Vanguard, and Angstrom Designs and the dedicated efforts of the core MegaFlex team at OAG: Mark McClenathen, Matt Menna, Robby Nielsen, David Langan, Peter Sorensen and Tom Trautt…plus all of the support from our entire Orbital ATK team in Goleta and San Diego.

References

[1]Tyson. N., *Space Chronicles, Facing the Ultimate Frontier*, W. W. Norton and Company, New York, 2012, p. 165.

[2]Murphy, D., "The SCARLET Solar Array: Technology Validation and Flight Results," *Deep Space 1 Technology Validation Symposium*, Pasadena, CA, February 2000.

[3]Rayman, M., et al., Dawn: "A Mission in Development for Exploration of Main Belt Asteroids Vesta and Ceres," *International Astronautical Congress*, IAC-04-Q.5.05, Vancover, Canada, October 2004.

[4]Vision and Voyages for Planetary Science in the Decade 2013-2022, Committee on the Planetary Science Decadal Survey, Space Studies Board, ISBN-10: 0-309-20954-4, March 2011.

[5]Kerslake, T., et al., "Solar Electric Propulsion Tug Power System Considerations," S*pace Power Workshop, Power Systems Architecture*, Los Angeles, CA, April 2011.

[6]Brophy, J., et al., "300-kW Solar Electric Propulsion System Configuration for Human Exploration of Near-Earth Asteroids," AIAA-2011-5514, *47th AIAA/ASME/ SAE/ASEE Joint Propulsion Conference*, August 2011.

[7]Capadona, L., et al., "Feasibility of Large High-Powered Solar Electric Propulsion Vehicles: Issues and Solutions," *AIAA Space 2011* Conference, Long Beach, CA, September 2011.

[8]Mercer, C., et al., "Benefits of Power and Propulsion Technology for a Piloted Electric Vehicle to an Asteroid," *AIAA Space 2011 Conference*, Long Beach, CA, September 2011.

[9]Solar Electric Propulsion System Demonstration Mission Concept Studies, Exploration Systems Mission Directorate BAA NNC11ZMA017K, Released June 21, 2011, awards posted September 20, 2011.

[10]Murphy, D., et al., "UltraFlex and MegaFlex – Development of Highly Scalable Solar Power," *42nd IEEE Photovoltaic Specialists Conference*, New Orleans, LA, June 2015.

[11]Technology Development for Solar Array Systems in Support of Electric Propulsion, Game Changing Opportunities in Technology Development, NASA Research Announcement NNL12A3001N, modified March 30, 2012.

[12]Murphy, D., "MegaFlex – The Scaling Potential of UltraFlex," AIAA-2012-1581, *53rd AIAA/ASME/ASCE/ AHS/ASC Structures, Structural Dynamics & Materials Conference, 13th Gossamer Spacecraft Forum*, Honolulu, HI, April 2012.

[13]Website for NASA-GRC Space Power Facility. URL: http://facilities.grc.nasa.gov/spf/index.html [cited December 2015].

[14]Deininger, W., et al., "Solar Electric Propulsion Demonstration Mission Baseline Concept Description," IEPC-2013-457, *33rd International Electric Propulsion Conference*, The George Washington University, Washington, D.C., October 2013.

[15]Deininger, W., et al., "Solar Electric Propulsion Demonstration Mission 30 kW-Class Concept Description," Paper No. 2628, *2014 IEEE Aerospace Conference*, Big Sky, MT, March 2014.

[16]Deininger, W., et al., "Solar Electric Propulsion Demonstration Mission Using a Minotaur IV Launch Vehicle," *50th AIAA/ASME/SAE/ASEE Joint Propulsion Conference*, Cleveland, OH, July 2014.

[17]McDonald, M., et al., "Extensibility of Human Asteroid Mission to Mars and Other Destinations," *AIAA SpaceOps*; Pasadena, CA, May 2014.

[18]Deininger, W., et al., "A Direct Drive Experiment as Part of a SEP Technology Demonstration Mission," *50th AIAA/ASME/SAE/ASEE Joint Propulsion Conference*, Cleveland, OH, July 2014.

[19]Human Exploration of Mars, Design Reference Architecture 5.0, Addendum, (Ref. Sec. 3.7.4.3 Autonomous Deployment), Mars Architecture Steering Group, NASA/SP-2009-566-ADD, B. Drake (editor), NASA Johnson Space Center, Houston, TX, July 2009.